Journal of Integrative Neuroscience

IMR Press

Original Research

# Comprehensive analysis of lncRNA expression profiles in rats with cerebral ischemia-reperfusion injury after treatment with 20(*R*)-ginsenoside Rg3

Yuan Yang[1,†], Bo He[1,†], Renhua Yang[1], Deyun Chen[1], Xiaochao Zhang[1], Fajing Li[1], Zhiqiang Shen[1,*], Peng Chen[1,*]

[1] *School of Pharmaceutical Sciences and Yunnan Key Laboratory of Pharmacology for Natural Products, Kunming Medical University, 650500 Kunming, Yunnan, China*

*Correspondence: shzhq21cn@aliyun.com (Zhiqiang Shen); chenpeng@kmmu.edu.cn (Peng Chen)
†These authors contributed equally.

DOI:10.31083/j.jin2101016



Submitted: 23 June 2021 Revised: 27 July 2021 Accepted: 17 August 2021 Published: 28 January 2022

This study was aimed at investigating the differentially expressions of long noncoding RNAs (lncRNAs) and mRNAs in the brains of a middle cerebral artery occlusion/reperfusion (MCAO/R) group and a MCAO/R + 20(*R*)-Rg3 group. Biological enrichment analysis was performed, and a lncRNA-mRNA coexpression network was constructed, to reveal the targets and pathways of 20(*R*)-Rg3 involved in the regulation of cerebral ischemia-reperfusion injury (CIRI). The RNA-seq high-throughput sequencing method was employed to detect differentially-expressed genes between the groups, which were verified by RT-PCR. Functional enrichment analyses of Gene Ontology (GO) and Kyoto Encyclopedia of Genes and Genomes (KEGG) pathway were performed to explore the biological functions and relevant pathways. The coexpression network of the screened lncRNAs and mRNAs was built by using Cytoscape software. The results identified 77 upregulated lncRNAs, 162 downregulated lncRNAs, 66 upregulated mRNAs and 472 downregulated mRNAs in the MCAO/R + 20(*R*)-Rg3 group, compared with those in the MCAO/R group. GO enrichment analysis showed that the GO terms were mainly enriched in stimulation response, cellular response, and stress response. KEGG pathways were mainly related to the tumor necrosis factor (TNF), NF-$\kappa$B, cytokine, and other receptor signaling pathways. In addition, the coexpression analysis between lncRNA and mRNA identified 314 nodes and 515 connections between 6 lncRNAs and 308 mRNAs, of which 511 were positive and 4 were negative. Among them, ENSRNOG-00000059555 was strongly correlated with AABR07001160.1. This study revealed multiple lncRNAs were involved in the neuroprotection of 20(*R*)-Rg3 against CIRI and thereby provided new insights into the use of 20(*R*)-Rg3 as a novel neuro protectant in ischemic stroke management.

*Keywords*

Cerebral ischemia-reperfusion injury; 20(*R*)-ginsenoside Rg3; lncRNA; mRNA; Coexpression network

## 1. Introduction

Ischemic stroke (also called cerebral infarction) is recognized as one of the most prevalent neurological/stroke-related disorders worldwide with high rates of morbidity and disability. Every year, an estimated 6.2 million people die of stroke, while the lifetime risk of stroke is approximately 8% to 10%. It has been reported that ischemic stroke makes up to 70–85% of all strokes [1]. Cerebral ischemia-reperfusion injury (CIRI) is considered as a complicated pathophysiological condition of ischemic stroke involving excitotoxicity, inflammatory response, oxidative stress and apoptosis [2]. The occurrence of CIRI can cause an imbalance in calcium homeostasis, resulting in excessive release of the neurotransmitter glutamate and excitatory amino acid toxicity [3]. In addition, CIRI can activate macrophages and microglia, produce proinflammatory mediators such as tumor necrosis factor (TNF), the interleukin family cytokines, and adhesion molecules, increase leukocyte infiltration, and eventually lead to the apoptosis of neurons [4]. At present, long noncoding RNAs (lncRNAs), as new key regulators involved in nervous system diseases, have attracted increasing attention from researchers [5].

Around 99% of mammalian genomes are pervasively transcribed into noncoding RNAs (ncRNAs), and most of which are lncRNAs [6]. LncRNAs can regulate target gene expression by affecting histone modification, chromatin remodeling and protein functional activity [7]. Accumulating research indicates that the function of lncRNAs is closely correlated with the pathological process of ischemic stroke [8]. It has been reported that overexpression of antisense noncoding RNA in the INK4 locus (ANRIL) alleviated PC-12 cell injury induced by oxygen-glucose deprivation (OGD), and the underlying mechanism maybe related to the suppressed miR-127, which is negatively regulated by expression of the anti-apoptotic factor myeloid leukemia factor (Mcl-1) [9]. Zhang *et al.* [10] found that knockdown of the lncRNA small nucleolar RNA host gene 6 (SNHG6) can reduce brain infarct volumes and alleviate neurobehavioral outcomes in mice following middle cerebral artery occlusion (MCAO). In addition, cell experiments confirmed that interfering with SNHG6 expression can reduce the expression of caspase-3, inhibit cell apoptosis, and increase the survival rate of cortical neurons

after OGD treatment. Therefore, by studying the interactions between lncRNAs and mRNAs, we can better understand the pathophysiological processes of CIRI and develop new therapeutic strategies for CIRI.

Studies have shown that the most active plant-derived natural products, such as saponins, flavonoids and alkaloids, have protective effects or potential activities against cerebral ischemia and are also important sources for preventing and treating ischemic stroke [11]. *Radix notoginseng* is the dried root of *Panax notoginseng* (Burk.) F.H. Chen, and its main active ingredients are dammarane-type triterpenoid saponins. Ginsenoside Rg3, the monomer saponin extracted from *P. notoginseng*, exists in two stereoisomeric configurations in nature, namely, 20(*S*)-Rg3 and 20(*R*)-Rg3. Pharmacological experiments confirmed that 20(*R*)-Rg3 has neuroprotective, antitumor and antioxidant properties [12–14]. Our previous research showed that 20(*R*)-Rg3 protects against CIRI in the rat brain by reducing the infarct rate and decreasing cerebral infarct volumes on 2,3,5-triphenyltetrazolium chloride (TTC)-stained brain sections, and improving the animals' behavior. In addition, 20(*R*)-Rg3 significantly suppressed caspase-3 and calpain I mRNA expression [15]. Also, *in vitro* experiments confirmed that 20(*R*)-Rg3 can reduce the apoptosis rate induced by OGD/R in SH-SY5Y cells, and the mechanism may have relations with the downregulation of Bax expression and the upregulation of Bcl-2 expression [16]. Current reports on 20(*R*)-Rg3 for treating neurological conditions tend to focus on a single therapeutic target or single molecular signaling pathway. The underlying mechanism of 20(*R*)-Rg3 based on multiple regulatory aspects and levels, especially lncRNAs, has not been completely illuminated.

In this study, we set out to investigate the changes in the lncRNA and mRNA expression profiles in a MCAO/R + 20(*R*)-Rg3 vs. a MCAO/R group by using RNA sequencing technology. Our results demonstrated that multiple lncRNAs are closely associated with the protective efficacy of 20(*R*)-Rg3 in a MCAO/R-induced rat model and therefore provide a novel treatment for neurological diseases related to ischemic stroke.

## 2. Materials and methods

### *2.1 Drugs and reagents*

20(*R*)-Rg3 (purity >99%) was generously supplied by Professor Cheng Zou (Kunming Medical University, Kunming, China). 20(*R*)-Rg3 (50 mg/mL) was dissolved in dimethyl sulfoxide (DMSO), mixed with 10% Tween 80 for solubilizing, and diluted to 20 mg/mL with normal saline. TRIzol reagent was obtained from Ambion (Austin, TX, USA). The reverse transcription (RT) kit was purchased from Thermo Fisher Scientific (Massachusetts, USA), and the fluorescent quantitative reagent was obtained from Roche Diagnosis Ltd. (Shanghai, China). The primers were synthesized by Wuhan Qingke Biotechnology Co., Ltd. (Wuhan, China). The other reagents and chemicals were of analytical grade.

### *2.2 Animal experiment and sample collection*

#### *2.2.1 Experimental animals*

Male Sprague-Dawley rats in a SPF-grade weighing about 300 g were purchased from the Laboratory Animal Center of Kunming Medical University [license number: SCXK (Yunnan) k2015-0002]. Rats were housed in a controlled environment maintained at 21–23 °C and 55% humidity. The animals were randomly divided into the MCAO/R group and MCAO/R + 20(*R*)-Rg3 group, with 8 rats in each group. After reperfusion for 24 h following ischemia for 2 h, the rats were euthanized, and brain tissue was collected. All animal procedures were performed in accordance with the Chinese legislation for animal use and experimentation and approved by the ethics committee from Kunming Medical University.

#### *2.2.2 MCAO/R model*

The rat model of MCAO/R was duplicated as reported previously [15]. Thereafter, the rats were scored according to the method of Bederson's test [17], and those rats that scored more than 3 points were considered as successful models. Briefly, the rats were anesthetized using 2% isoflurane and fixed in the supine position, and cervical hair was removed with a razor. Then, a small incision of approximately 3.0 cm was cut along the medioventral line. The right common carotid artery, external carotid artery and internal carotid artery were bluntly separated, and the proximal and external carotid arteries were ligated. A 0.47 mm nylon thread was inserted into the middle cerebral artery at a depth of approximately 20 mm. During the operation, the rats were placed on the heating pad, and the filament was withdrawn after two hours of ischemia/24 h of reperfusion. The therapeutic agent of 20(*R*)-Rg3 (20 mg/kg, i.p.) was given 12 h before the operation. Two hours later, the thread was retracted to perform the reperfusion operation, and the agent was immediately given a second time. Twelve hours after reperfusion, the last dosage of 20(*R*)-Rg3 was given. The experimental animals were euthanized 24 h after reperfusion, and the brain tissues were rapidly collected.

### *2.3 LncRNA and mRNA sequencing analysis*

The cerebral cortex was collected from three randomly selected rats in each group, and a 2 × 2 × 2 mm section from the ipsilateral ischemic penumbra was isolated, placed into TRIzol reagent and immediately prepared for sequencing. Ribosomal RNA was removed from the total RNA. The purified double-stranded complementary DNA (cDNA) was subjected to terminal repair, tailing and ligation to a sequencing adapter. cDNA (200 bp) was purified with AMPure XP beads, and PCR amplification was carried out to obtain the library. After obtaining the RNA-seq data, quality control and screening of the original data were carried out, and the RNA-seq data were compared and analyzed using Hisat 2 software (v2.0.5, http://ccb.jhu.edu/software/hisat2).

**Table 1. Primer sequences for real-time quantitative PCR.**

| Gene | Forward primer | Reverse primer | Length (bp) | TM (°C) |
|---|---|---|---|---|
| *GAPDH* | GGGTGTGAACCACGAGAAAT | ACTGTGGTCATGAGCCCTTC | 20 | 59.7 |
| *Ephx2* | CGTTCGACCTTGACGGAGTG | CTGGAAAGCGCCAAGTAGGA | 20 | 57.4 |
| *Phyhip* | CTCTCTCTTCTTGCGCGTTC | GATGATGAGCTCTCCAGGCAG | 21 | 57.4 |
| *Hspa1b* | CAGCGAGGCTGACAAGAAGA | TTGCAGACCGAACGAAGGAG | 20 | 59.5 |
| *Itga2* | ACCCTTTGGATCTGCGAGTG | AGAAAACTCAGCCAGGACGG | 20 | 57.4 |
| *Ptx3* | GCAGCCAAGGACAGGTAGTT | ACCCCTGTGATGGTCTTAGC | 20 | 57.4 |
| *Mettl27* | GGGAGGCTGAGACAGGAGGA | GTCACCATATTGATGCCGAACT | 22 | 59.5 |
| *Cyp23* | CTCCAGTTGAACCAGCACCA | GAAGACCCAGAAATGAACCCAC | 22 | 57.4 |
| *Msn* | GCACAAGTCTGGCTACCTGG | GTCAGCTTTGTCTGCTACCCA | 21 | 57.4 |

GAPDH, glyceraldehyde-3-phosphate dehydrogenase; Ephx2, Epoxide hydratase2; Phyhip, Alkate oxidase; Hspa1b, Heat Shock 70kDa Egg 1B; Itga2, Integrin A2; Ptx3, Pentraxin 3; Mettl27, Methyltransferase like 27; Cyp23, Cytochrome oxidase23; membrane protein pseudogene (Msn) is a membrane protein.

### *2.4 Differential expression analysis of mRNAs and lncRNAs*

The differential expression of each lncRNA and mRNA in each sample were analyzed using Cuffdiff software (v2.2.1, http://cole-trapnell-lab.github.io/cufflinks/install/). A fold change value of 1.3 with a *p*-value of 0.05 was used as the cutoff, and padj less than 0.05 indicated a significant difference.

### *2.5 RT-PCR*

RT-PCR was used to validate the differentially expressed genes. Fresh brain tissue was immediately immersed in TRIzol reagent. After chloroform phase separation, RNA was extracted from the upper transparent layer. Total RNA was reverse transcribed, and RT-PCR was performed using a real-time PCR system (ABI7500; Applied Biosystems). Glyceraldehyde-3-phosphate dehydrogenase (GAPDH) was regarded as an internal reference control, and the comparative cycle threshold (Ct) method was used for the relative quantitative analysis [18]. The primer sequences are listed in Table 1.

### *2.6 GO and KEGG enrichment analysis*

Pathway enrichment analysis was used to identify the major signal transduction and biochemical metabolic pathways associated with differentially expressed genes (DEGs). Gene Ontology (GO) term enrichment was carried out using GOseq software to acquire annotation and enrichment information. The differentially expressed mRNAs were mapped to the appropriate GO database, and the number of genes was calculated for each term. The enrichment analysis of Kyoto Encyclopedia of Genes and Genomes (KEGG) pathway was conducted using KOBAS (v2.0, http://kobas.cbi.pku.edu.cn). The GO terms/pathways with significant enrichment were defined with $p < 0.05$ as thresholds.

### *2.7 LncRNA-mRNA coexpression network*

Based on correlation analysis of the differentially expressed lncRNAs and mRNAs, a coexpression network of 6 lncRNAs and 308 mRNAs was constructed by using weighted gene coexpression network analysis (WGCNA). The network was visualized using Cytoscape software (version 2.8.3; Cytoscape Consortium, San Diego, CA, USA). Six lncRNAs are represented by red squares, and 308 mRNAs are represented by blue nodes. The positive and negative connections are shown as solid lines and dotted lines, respectively.

### *2.8 Statistical analysis*

All analyses were performed using SPSS 20.0 (IBM Corp., Chicago, IL, USA). Results were expressed as the mean ± S.E.M. The two groups were compared using a two-tailed Student's *t*-test. Spearman correlation analysis was used to examine the relationship between mRNAs and lncRNAs. Significance was assumed for $p < 0.05$.

## 3. Results

### *3.1 Overview of RNA sequencing technology*

The quality-controlled library was sequenced by Illumina PE150 according to the data output requirements and effective concentration of the library. A total of 726,279,344 raw data points were generated (Table 2). After stringent quality assessment, a total of 708,340,346 clean reads were acquired. At the same time, the clean reads were compared with the reference genome to obtain transcriptome information, and the RNA-seq sequencing data were compared and analyzed by Hisat 2 software. The comparison rates of model 1, model 2, model 3, 20(*R*)-Rg3_1, 20(*R*)-Rg3_2, and 20(*R*)-Rg3_3 was 96.77%, 96.68%, 96.73%, 96.46%, 96.07% and 96.68%, respectively (Table 3). Overall, a total of 708,340,346 transcripts were collected, which were used for subsequent analysis.

### *3.2 Identification of lncRNA*

The single-exon transcripts with low credibility in the transcriptional results were filtered out using Cuffcompare software (v2.2.1, http://cole-trapnell-lab.github.io/cufflinks/install/). Transcripts greater than 200 bp in length and exon number ≥2 were selected as lncRNA candidates. For the screening and confirmation of lncRNAs, the software programs CPC2, Pfam and CNCI were used. The intersection of transcripts with no coding potential in these software analytic results was selected to obtain 7804 novel lncRNAs and 392 novel mRNAs. According to their location with re-

**Table 2. Summary of data quality ($n = 3$).**

| Sample name | Raw reads | Clean reads |
|---|---|---|
| Model 1 | 137,917,586 | 134,670,272 |
| Model 2 | 135,458,378 | 132,972,226 |
| Model 3 | 117,303,944 | 113,125,424 |
| Rg3_1 | 138,741,702 | 136,323,788 |
| Rg3_2 | 101,383,840 | 98,266,784 |
| Rg3_3 | 95,473,894 | 92,981,852 |

Model group was the middle cerebral artery occlusion/reperfusion (MCAO/R) model group. Rg3 group was 20(*R*)-ginsenoside Rg3 group (20 mg/kg).

spect to known mRNAs based on the HGNC guidelines, the newly identified lncRNAs were categorized based on the four types as follows: 1249 antisense lncRNAs, 5354 lncRNAs, 1201 sense overlapping lncRNAs and 0 sense intronic lncRNAs (Fig. 1). In addition, 3571 protein-coding transcripts were identified. The transcripts of 7804 lncRNAs and 3571 protein-encoded genes were further analyzed.

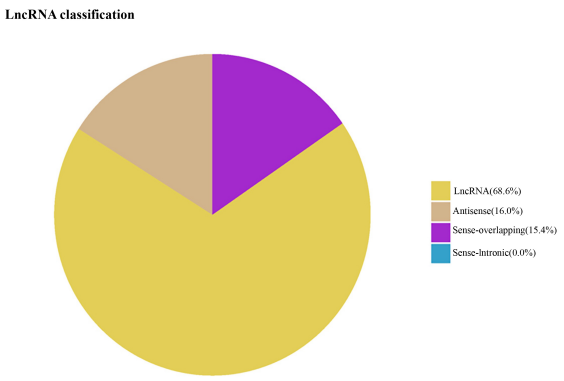


**Fig. 1. Venn distribution of different lncRNA types.** LncRNA, antisense, sense-overlapping, and sense-intronic were presented as yellow, brown, purple and green, respectively.

### *3.3 Comparison of lncRNA and mRNA characteristics*

The predicted 11,375 lncRNAs and 3571 mRNAs were used for comparison with known lncRNAs and mRNAs. The results demonstrated that the average transcript lengths of mRNAs were longer than those of lncRNAs (Fig. 2a), and most mRNAs contained more exons than lncRNAs (Fig. 2b). The open reading frame lengths of mRNAs in the obtained dataset were longer than those of lncRNAs (Fig. 2c). All lncRNAs overlapped with known lncRNAs. The above results suggested that the predicted novel lncRNAs were similar to known lncRNAs and significantly different from known mRNAs.

### *3.4 Differential expression analysis of lncRNA and mRNA*

The fold change cutoff value was set at 1.3, and the differential expression was analyzed by using Cuffdiff software (v2.2.1, http://cole-trapnell-lab.github.io/cufflinks/install/) ($p < 0.05$). The results are shown in two forms: a volcano map and a cluster analysis map. 239 lncRNAs and 538 mRNA transcripts were identified as significantly differential expressions in the MCAO/R + 20(*R*)-Rg3 group compared with those in the MCAO/R group. There were 77 upregulated and 162 downregulated lncRNAs ($p < 0.05$, Fig. 3a), and 66 upregulated and 472 downregulated mRNA transcripts among the above differentially expressed RNAs ($p < 0.05$, Fig. 3b). Cluster analysis showed similar results to the volcano map (Fig. 3c,d).

### *3.5 Verification of differentially expressed lncRNA and mRNA genes*

Among lncRNA and mRNA transcripts with significant differential expression, four lncRNAs and four mRNAs were chosen randomly and verified by RT-PCR. As shown in Fig. 4, compared with that in the MCAO/R group, the expression of the lncRNAs Mettl27 and Cyp23 in the MCAO/R + 20(*R*)-Rg3 group was upregulated ($p < 0.01$), whereas the expression of the lncRNAs Msn and Ptx3 was downregulated ($p < 0.01$, $p < 0.05$). In the MCAO/R + 20(*R*)-Rg3 group, a significant decrease in the mRNA expression of Hspa1b and Itga2 ($p < 0.01$, $p < 0.05$), and a significant increase in the mRNA expression of Ephx2 and Phyhip, compared with the MCAO/R group ($p < 0.01$, $p < 0.05$). The results of RT-PCR were consistent with those of RNA sequencing data, confirming the reliability of sequencing.

### *3.6 Functional enrichment analyses: GO and KEGG*

All the differentially-expressed genes were enriched and analyzed. After classifying the enriched GO terms, a histogram of GO enrichment analysis was generated. The histogram showed that the top five significant GO terms were stimulation response (GO: 00508960), cell immunity activation response (GO: 00051716), biological positive regulatory response (GO: 0045321), stress response (GO: 0006950), and molecular function regulation (GO: 0065009) (Fig. 5a). KEGG analysis showed that the top seven signaling pathways involved in the regulation of CIRI by 20(*R*)-Rg3 were the pathways for tuberculosis, proteoglycan, osteoclast differentiation, phagocyte, TNF, NF$\kappa$B, and cytokine receptors (Fig. 5b). Our results indicate that 20(*R*)-Rg3 may exert a protective role against CIRI at multiple regulatory aspects and levels.

### *3.7 Construction of lncRNA-mRNA coexpression network*

On the basis of the above related differential gene analysis, the lncRNA-mRNA coexpression network was constructed by selecting lncRNA-mRNA pairs with an absolute value of the correlation coefficient (|correlation|, |cor|) $\geq$0.9 and $p <$ 0.05. 6 differentially expressed lncRNAs and 308 interacting mRNAs were selected to construct the lncRNA-mRNA network, which contained 314 nodes and 515 connections (511 positive connections and 4 negative connections) between these lncRNAs and mRNAs. Among them, a strong interaction was identified between ENSRNOG-00000059555 and AABR07001160.1 based on a Pearson correlation coefficient (PCC) of 0.984 (Fig. 6).

**Table 3. Comparison of samples based on total reads and total mapped ($n$ = 3).**

| Sample name | Model 1 | Model 2 | Model 3 | Rg3_1 | Rg3_2 | Rg3_3 |
|---|---|---|---|---|---|---|
| Total reads | 134,670,272 | 132,972,226 | 113,125,424 | 136,323,788 | 98,266,784 | 92,981,852 |
| Total mapped | 130,326,512 (96.77%) | 128,563,463 (96.68%) | 1,109,431,654 (96.73%) | 131,497,694 (96.46%) | 94,407,835 (96.07%) | 89,892,005 (96.68%) |

Model group was the middle cerebral artery occlusion/reperfusion (MCAO/R) model group. Rg3 group was 20(*R*)-ginsenoside Rg3 group (20 mg/kg).

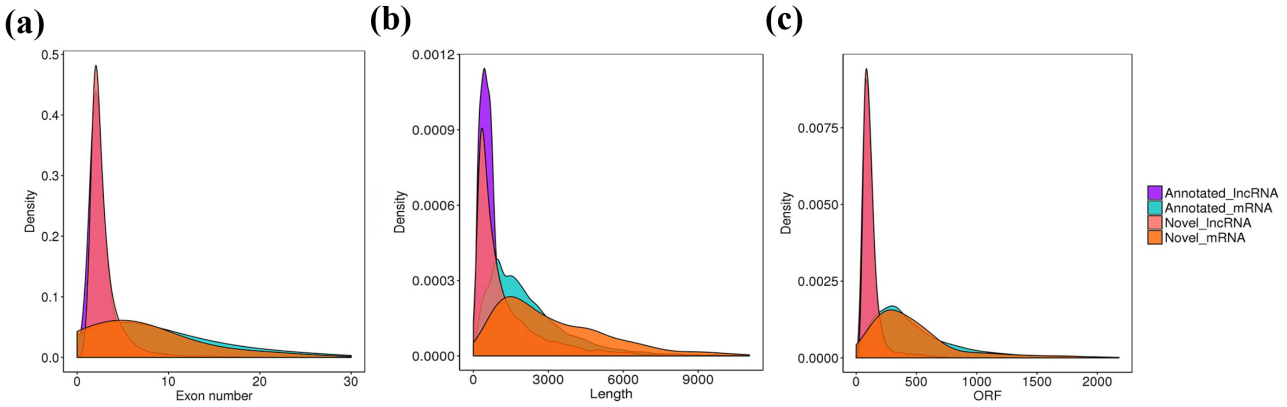


**Fig. 2. Comparing the characteristics of lncRNA and mRNA.** (a) Transcription length distribution in mRNA and lncRNA. (b) The distribution of exon number of mRNA and lncRNA. (c) Distribution of open reading frame length in mRNA and lncRNA. Purple region indicates the known lncRNAs, the cyan region reflects the known mRNAs, the red region indicates the predicted new lncRNAs, and the orange region represents the predicted new mRNAs ($n$ = 3).

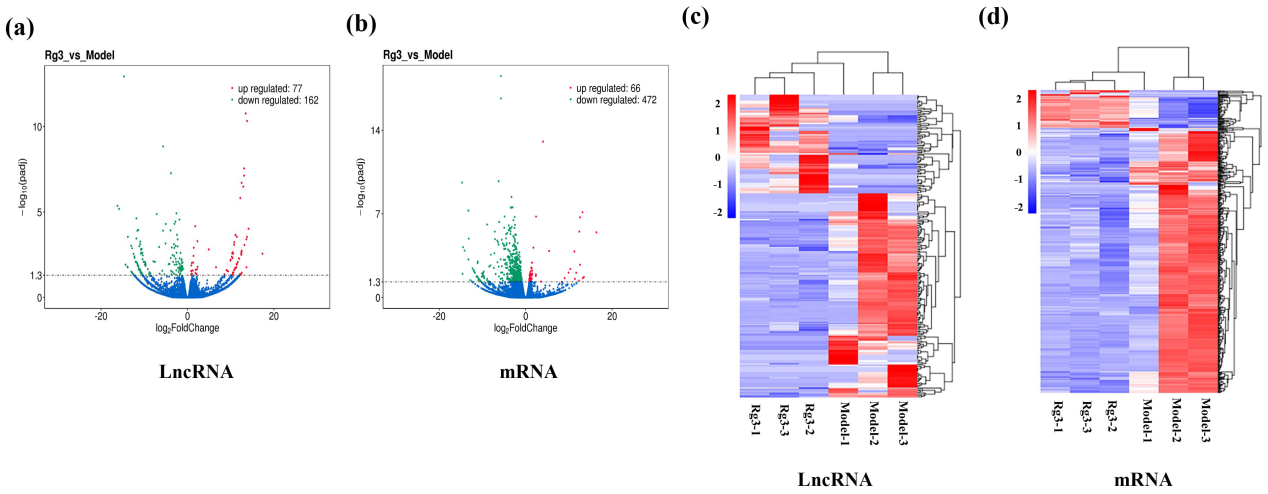


**Fig. 3. Differential expression analysis of lncRNA and mRNA.** (a,b) The abscissa represents the expression multiple Change (log2 Fold Change) between different samples or comparison combinations. The ordinate represents the level of significance of the expression difference. The up-regulated genes are represented by red dots, down-regulated genes are represented by green dots, and the genes with no significant changes are represented by blue dots. (c,d) The horizontal axis denotes each sample, and the vertical axis represents the differentially expressed genes. The selected genes were clustered on the left side of the dendrogram according to the degree of similarity, and clustering of each sample was performed on the top side according to the expression similarity degree. Color scale represents the expression level of each sample from low expression level (blue) to high expression level (red).

## 4. Discussion

Ischemic stroke is an acute attack of neurological dysfunction caused by focal cerebral ischemia and is the second major cause of death worldwide [19]. The clinical treatment of ischemic stroke mainly aims to restore blood flow as soon as possible, but at the same time, resulting in CIRI, which can cause a series of serious cascade reactions, such as blood-brain barrier dysfunction, oxidative stress, excitotoxicity, and inflammation after ischemia, and can eventually lead to neuronal death [20]. Some researchers have elucidated the changes of lncRNA, microRNA (miRNA) and mRNA expression profiles in focal ischemic rat brains by using RNA sequencing technology. A coexpression network analysis revealed that 1924 new lncRNAs may be involved in brain injury and DNA repair [21]. Recent studies using RNA-seq, a microarray sequencing technology, showed that lncRNAs

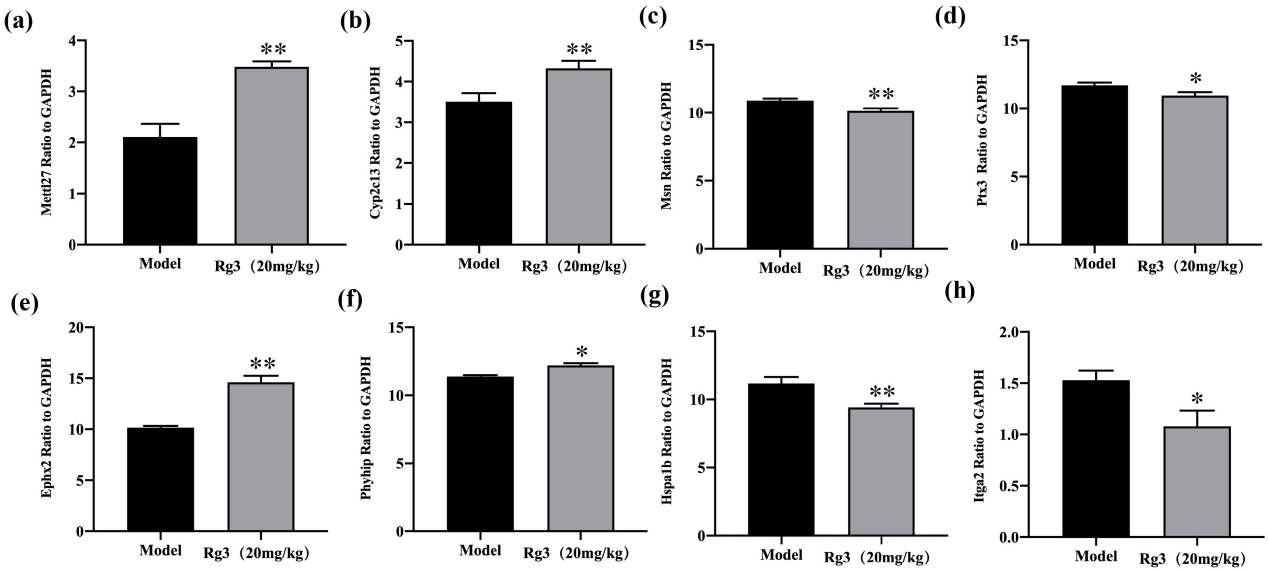


**Fig. 4. RT-PCR Verification of differentially expressed genes of lncRNA and mRNA.** (a) The expression of Mettl27. (b) The expression of Cyp23. (c) The expression of Msn. (d) The expression of Ptx3. (e) The expression of Ephx2. (f) The expression of Phyhip. (g) The expression of Hspa1b. (h) The expression of Itga2. Model group represents the MCAO/R group, and Rg3 (20 mg/kg) group donates MCAO/R 20(*R*)-Rg3 group. Glyceraldehyde-3-phosphate dehydrogenase (GAPDH) was used as a control housekeeper gene, Mean ± S.E.M., $n = 8$. $^{*}p < 0.05$, $^{**}p < 0.0$l vs. model group.

play critical roles in multiple diseases. Bao *et al.* [22] found that a large number of abnormally expressed lncRNAs were screened from ischemic stroke patients and animals with ischemic injury: MEG3, H19 and MALAT1 may be involved in neurogenesis, angiogenesis, and inflammation through gene regulatory mechanisms include DNA transcription, methylation, RNA folding, and gene imprinting. Prior researchers have studied the expression profiles of lncRNA in normal and ischemic stroke models. In this study, we performed systematic analyses of lncRNA and mRNA expression profiles from an untreated MCAO/R group and a treated MCAO/R + 20(*R*)-Rg3 group, using sequencing technology. It was found that 20(*R*)-Rg3 protects against CIRI by regulating 239 differentially expressed lncRNAs (77 upregulated, 162 downregulated) and 538 differentially expressed mRNAs (66 upregulated, 472 downregulated) involved in stimulus response (GO: 00508960), cell immunity activation response (GO: 00051716), stress response (GO: 0006950), etc. The lncRNA-mRNA coexpression network showed that there was a strong correlation between ENSRNOG00000095 and AABR07001160.1 in the MCAO/R rat model after 20(*R*)-Rg3 treatment.

RNA-seq technology can provide gene expression information at the transcription level, which can be used to infer the function of unknown genes and reveal the regulatory mechanism of specific genes [23]. Studies have indicated that some aberrantly expressed lncRNAs and their gene polymorphisms in ischemic stroke patients can be developed as potential serum diagnostic marker of ischemic stroke [24]. Deng *et al.* [25] found that expressions of the lncRNAs SNHG15, linc-DHFRL1-4, and linc-FAM98A-3 in the serum of patients with ischemic stroke were significantly increased compared with the serum of healthy controls. Moreover, their expression changes were significantly associated with neurological deficits and could be proposed as potential biomarkers for ischemic stroke. In the present study, we detected a total of 11,375 differentially expressed lncRNAs and 3571 differentially expressed mRNAs between the 20(*R*)-Rg3 treated group and the untreated MCAO/R model group, using RNA-seq technology, of which 239 lncRNAs and 538 mRNAs showed statistically significant differences. To verify the reliability of the sequencing results, four lncRNAs and four mRNAs with significant differences were selected for RT-PCR. The results of RT-PCR agreed well with the sequencing results, indicating that the sequencing results were highly reliable.

In the pathological process of CIRI, severe ischemia triggers oxidative stress and the inflammatory response of brain tissue and nerve cells through the increased production of free radicals and calcium overload [26]. After CIRI, the dynamic imbalance in the nervous system between oxidative factors such as reactive nitrides (RNS) and reactive oxygen species (ROS), and antioxidant factors such as superoxide glutathione (GSH) and dismutase (SOD), causes nerve cell injury and eventually leads to brain nerve dysfunction [27]. Studies have demonstrated that various signaling pathways were involved in the regulation of oxidative stress, including the Kelch-like ECH-associated protein 1/nuclear factor erythroid 2-related factor 2 (Keap1/Nrf2) pathway, the phosphatidylinositol-3-kinase/protein kinase B (PI3K/Akt)

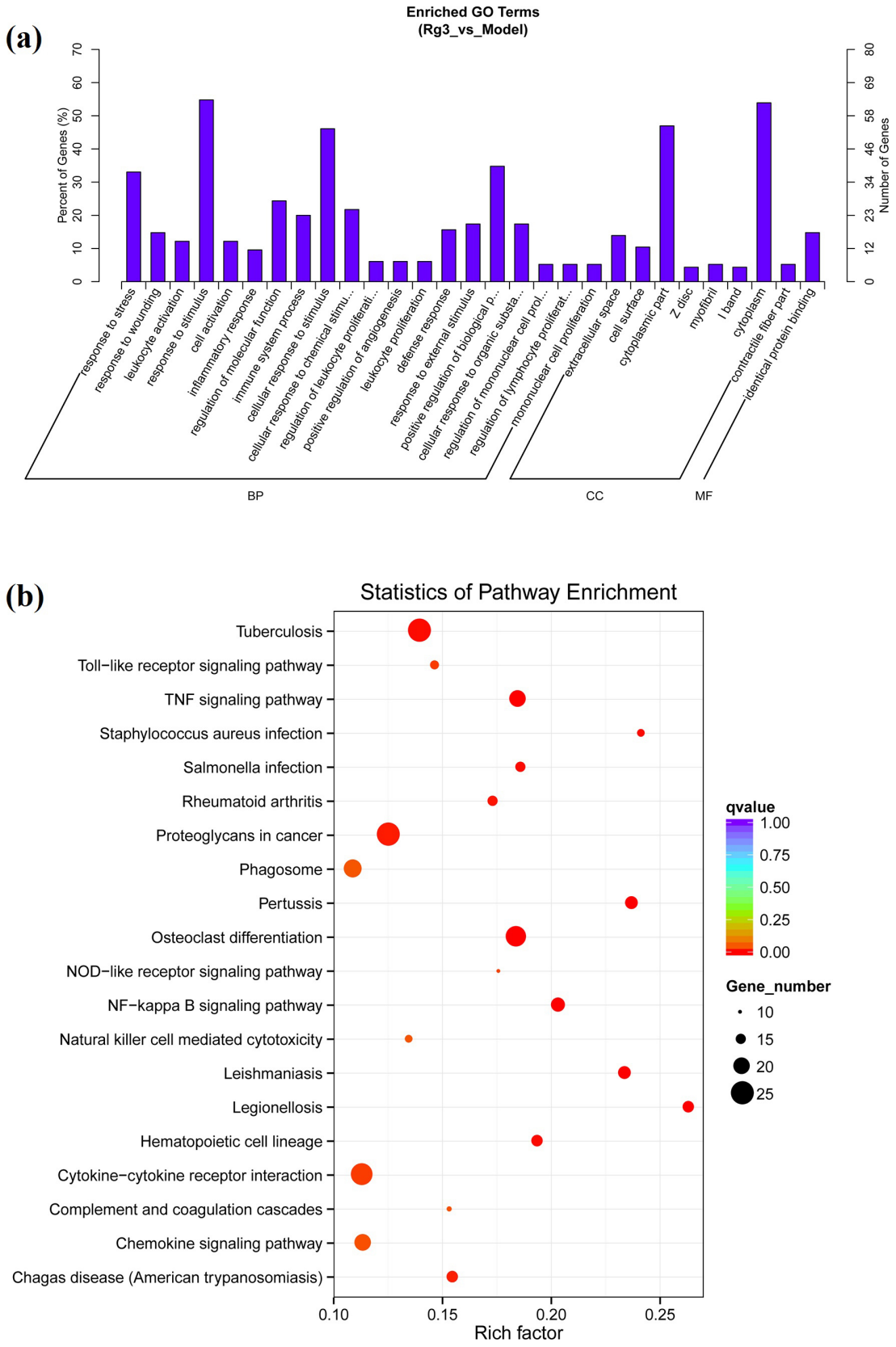


**Fig. 5. GO and KEGG pathway enrichment analysis.** (a) GO enrichment. (b) KEGG pathway enrichment. The vertical axis represents different pathways, and the horizontal axis represents the proportion of the differentially expressed genes. The redder color of the dots represents the more significant enrichment. The size of the circle indicates the number of genes enriched in the pathway.

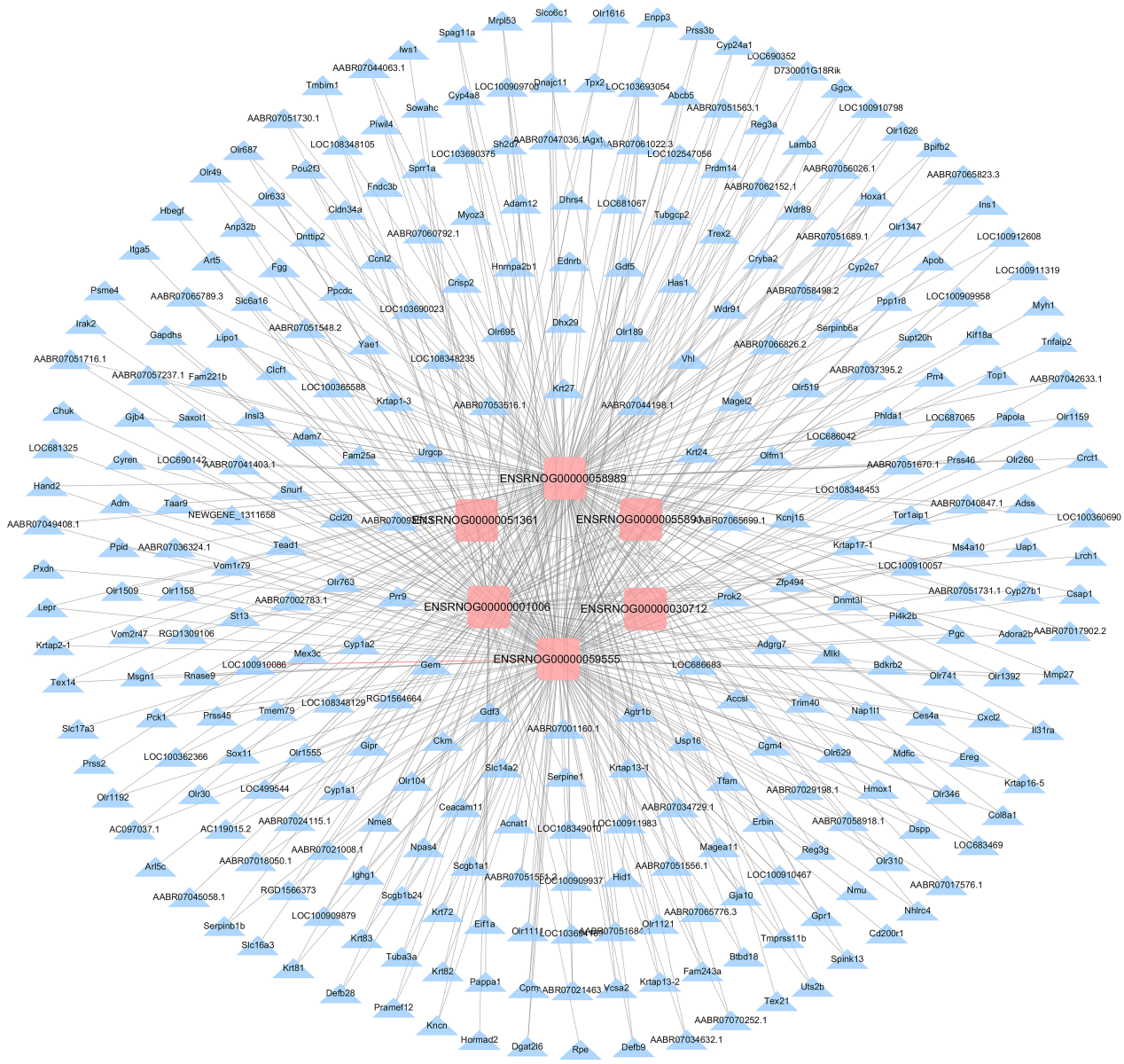


**Fig. 6. LncRNA-mRNA co-expression network.** In the network analysis, the red and blue nodes represent the lncRNA and mRNA, respectively ($n$ = 3).

pathway, and the Wnt signaling pathway [28]. The Wnt signaling pathway also plays an important role in signal transduction in the brain. Oxidative stress can lead to Wnt signaling pathway dysfunction with subsequent alterations in neuronal apoptosis [29]. Yao *et al.* [30] found that the lncRNA LOC101927196 can reduce oxidative stress *via* suppression of the Wnt signaling pathway by targeting frizzled class receptor 3 (FZD3) in a rat model of autism.

In addition, the forkhead frame transcription factor family O subgroup (FOXO) is an important mediator of the intracellular stress response by inducing the expression of antioxidant genes and subsequently activating antioxidant enzymes in response to oxidative stress [31]. FOXO3, a member of the FOXO family, can regulate the activity of various transcription factors and participate in cell apoptosis. It has been reported that FOXO3 can initiate transcription of the downstream antioxidant stress genes manganese superoxide dismutase (MnSOD) and catalase genes. Some studies have reported that FOXO3 overexpression can induce the activation of autophagy and protect neurons from oxidative stress [32]. It has been confirmed that lncRNAs has a crucial function in oxidative stress injury by regulating the FOXO3 signaling pathway. Wen *et al.* [33] showed that lncRNA LINC00963 promoted oxidative stress by activating the FOXO3 signaling pathway. Other studies have confirmed that upregulation of lncRNA SNHG12 expression can improve cell activity, inhibit oxidative stress and suppress the autophagy of HT22 cells by repressing the SIRT1/FOXO3 signaling pathway [34]. In the current study, GO enrichment analysis suggested that the effects of 20(*R*)-Rg3 on CIRI were related

to responses such as stimulation response (GO: 00508960), stress response (GO: 0006950) and cell immunity activation response (GO: 00051716). KEGG pathway analysis revealed that the Wnt pathway and the FOXO3 pathway were shown to participate to the protective effects of 20(*R*)-Rg3 against CIRI induced by MCAO/R, but the specific mechanism needs further experimental study.

CIRI can result in an increase in inflammatory mediators, such as TNF$\alpha$, interleukins (Ils) and hypoxia-inducible factor-1 (HIF-1), in ischemic regions [35]. Under the action of inflammatory factors, IKB kinases (IKKs) are activated and can in turn activate IKB$\alpha/\beta$ through serine phosphorylation at N-terminal residues. Subsequently, NF-$\kappa$B translocates into the nucleus, and the NF-$\kappa$B pathway is activated, which further promotes the inflammatory response [36]. Recent studies have shown that lncRNAs can also modulate CIRI pathological processes through regulation of the inflammatory reaction [37]. Studies have indicated that low expression of the lncRNA ANRIL can reduce cerebral infarction-induced neuronal apoptosis through suppressing the NF-$\kappa$B signaling pathway [38]. Other studies have demonstrated that silencing the lncRNA CaMK2D-associated transcript 1 (C2dat1) can reduce the expression of CaMK$\delta$ and potentiate Neuro-2a cell death in OGD/R-induced conditions, and the potential mechanism has been closely related to the suppression of the NF-$\kappa$B signaling pathway [39]. In our study, these inflammation-related signaling pathways, including the NF-$\kappa$B signaling pathway and TNF signaling pathway, were identified in the KEGG pathway analysis. Our results demonstrate that 20(*R*)-Rg3 may exert anti-inflammatory effect by affecting the NF-$\kappa$B signaling pathway and/or the TNF signaling pathway, and its potential molecular mechanism is worthy of further exploration.

The analysis of lncRNA-mRNA coexpression can help to further clarify the molecular regulatory mechanism by identifying the specific associated targets and their interactions. Previously, researchers collected blood from three healthy controls and three ischemic stroke patients and analyzed the lncRNA-mRNA coexpression network. Their results showed that LOC102723446 was coexpressed with lymphoid enhancer binding factor 1 (LEF1) and Kelch-like family member 3 (KLHL3), suggesting that LOC102723446 may contribute to ischemic stroke pathogenesis by regulating LEF1 and KLHL3 expression [40]. Wu *et al.* [41] constructed a lncRNA-mRNA coexpression network from a rat model of brain ischemia-reperfusion injury using genome-wide lncRNA microarray analysis. Their data showed that lncRNA N1LR inactivates the phosphorylation site of p53 to probably provide protection in ischemic stroke model. In the present study, we also constructed a lncRNA-mRNA coexpression network based on Pearson correlation analysis. The results showed that six lncRNAs, ENSRNOG00000058989, ENSRNOG0000005589, ENSRNOG00000051361, ENSRNOG00000010061, ENSRNOG00000059555, and ENSRNOG00000030721, interacted with 308 mRNAs. Taking six lncRNAs as the core, the closer the surrounding mRNAs were, the higher the correlation was. Among these mRNAs with high correlation, we found that many genes could regulate neurons, such as prokinetin 2 (Prok2), growth/differentiation factor 3 (GDF3) and C-C chemokine ligand 20 (CCL20). Among them, Prok2 is an indicator related to neuronal expression. Studies have found that neural stem cells in the subventricular zone of the lateral ventricle gave rise to new interneurons through the rostral migratory stream to the olfactory bulb (OB), and Prok2/ProkR2 signaling pathway plays a critical role in the radial and tangential migration of OB interneurons [42]. In addition, GDF3, a member of the large TGF-$\beta$/BMP/GDF superfamily, was highly expressed in the cerebral cortex, hippocampus, and cerebellum [43]. Li *et al.* [44] found that GDF3 could promote neuronal differentiation of neuron-like PC12 cells, which suggested that GDF3 is a key regulator of neuronal differentiation. CCL20, a chemokine of the subfamily of small CC cytokines, regulates cell chemotaxis, migration, and inflammation when it binds to the specific receptor CCR6. CCL20 gene expression in neurons and microglia was significantly upregulated in the acute stage after subarachnoid hemorrhage, and participated in the pathological process of early brain injury, such as the inflammatory response and neuronal apoptosis. Inhibition of CCL20 activity could significantly inhibit the pathological process of the inflammatory response and neuronal apoptosis, and alleviate the neurological dysfunction [45]. Based on the key Cytoscape findings, 20(*R*)-Rg3 may exert protective effect in regulating the expression of these genes, which is worthy of further investigation.

Nevertheless, there were some deficiencies in this study. Although we previously reported that 20(*R*)-Rg3 conferred an impressive protective effect against CIRI, we did not explore the functional/structural outcomes of 20(*R*)-Rg3 in brain tissue in this study, and the detailed mechanism of action of key target genes is also worthy of attention and further research. Another limitation of the present study is that a sham surgery group was not tested. However, we focused on the transcriptional expression profile of lncRNAs, regulated by 20(*R*)-Rg3 in CIRI, and complete lncRNA-mRNA coexpression analysis also found some meaningful results. We will conduct further studies on the functions and related pathways of these significantly regulated lncRNAs closely related to CIRI. Future research is expected to better reveal the regulatory mechanism of 20(*R*)-Rg3 in the control of CIRI at the molecular level.

## 5. Conclusions

In the present study, we performed a comprehensive analysis of lncRNAs and mRNAs expression profiles of in rats with CIRI treated with 20(*R*)-Rg3 and explored potential therapeutic targets for the treatment of CIRI. The data showed that 20(*R*)-Rg3 may work in the therapy of CIRI through anti-inflammatory and antioxidant pathways, in-

cluding the Wnt, FOXO3, NF-$\kappa$B, and TNF signaling pathways. These findings may offer novel insight for future studies on 20(*R*)-Rg3 as a potent candidate for CIRI treatment.

## Author contributions

YY and BH performed experiments and wrote the paper; RY, XZ analyzed the data; DC and FL performed the experimental animals; ZS revised article critically for important intellectual content; PC guided the experiment.

## Ethics approval and consent to participate

All experiments were conducted in accordance with the Chinese Legislation on the care and use of laboratory animals and approved by the Ethical Committee of Kunming Medical University, ethic code: SCXK (Yunnan) k2015-0002.


## Acknowledgment

We thank the anonymous reviewers for their valuable review of the article.

## Funding

This work was supported by the National Natural Science Foundation of China (No. 81660613, 81860665), the Joint Fund for the Department of Science and Technology of Yunnan Province-Kunming Medical University (No. 2019FE001-191, 202001AY070001-157), and the Ten-Thousand Talents Program of Yunnan Province (No. YNWR-QNBJ-2019-137).


## Conflict of interest

The authors declare no conflict of interest.

## References


[1] Lees KR, Bluhmki E, von Kummer R, Brott TG, Toni D, Grotta JC, *et al.* Time to treatment with intravenous alteplase and outcome in stroke: an updated pooled analysis of ECASS, ATLANTIS, NINDS, and EPITHET trials. The Lancet. 2010; 375: 1695–1703.

[2] Gao Y, Wen LL, Yang X, Wang J, Feng J. Pathological mechanism of focal cerebral ischemia and reperfusion injuries in mice. Journal of Biological Regulators and Homeostatic Agents. 2019; 33: 1507–1513.

[3] Zhang L, Zhang RL, Jiang Q, Ding G, Chopp M, Zhang ZG. Focal embolic cerebral ischemia in the rat. Nature Protocols. 2015; 10: 539–547.

[4] Laban H, Weigert A, Zink J, Elgheznawy A, Schürmann C, Günther L, *et al.* VASP regulates leukocyte infiltration, polarization, and vascular repair after ischemia. The Journal of Cell Biology. 2018; 217: 1503–1519.

[5] Clark BS, Blackshaw S. Long non-coding RNA-dependent transcriptional regulation in neuronal development and disease. Frontiers in Genetics. 2014; 5: 164.

[6] Wang Y, Pan W, Ge J, Wang X, Chen W, Luo X, *et al.* A review of the relationship between long noncoding RNA and post-stroke injury repair. Journal of International Medical Research. 2019; 47: 4619–4624.

[7] Jathar S, Kumar V, Srivastava J, Tripathi V. Technological Developments in lncRNA Biology. Advances in Experimental Medicine and Biology. 2017; 1008: 283–323.

[8] Dharap A, Nakka VP, Vemuganti R. Effect of focal ischemia on long noncoding RNAs. Stroke. 2012; 43: 2800–2802.

[9] Liu B, Cao W, Xue J. LncRNA ANRIL protects against oxygen and glucose deprivation (OGD)-induced injury in PC-12 cells: potential role in ischaemic stroke. Artificial Cells, Nanomedicine, and Biotechnology. 2019; 47: 1384–1395.

[10] Zhang X, Liu Z, Shu Q, Yuan S, Xing Z, Song J. LncRNA SNHG6 functions as a ceRNA to regulate neuronal cell apoptosis by modulating miR-181c-5p/BIM signalling in ischaemic stroke. Journal of Cellular and Molecular Medicine. 2019; 23: 6120–6130.

[11] Rehman MU, Wali AF, Ahmad A, Shakeel S, Rasool S, Ali R, *et al.* Neuroprotective Strategies for Neurological Disorders by Natural Products: an update. Current Neuropharmacology. 2019; 17: 247–267.

[12] Chen DY, Shen ZQ, He B. Research progress on pharmacological effect and mechanism of 20(*R*)-ginsenoside Rg3. Natural Product Research and Development. 2019; 31: 1285–1290.

[13] Che J, Liu Z, Ma H, Li Y, Zhao H, Li X, *et al.* Influence of as2O3 combined with ginsenosides Rg3 on inhibition of lung cancer NCI-H1299 cells and on subsistence of nude mice bearing hepatoma. Asian Pacific Journal of Tropical Medicine. 2014; 7: 772–775.

[14] Zhang Y, Yang X, Wang S, Song S. Ginsenoside Rg3 Prevents Cognitive Impairment by Improving Mitochondrial Dysfunction in the Rat Model of Alzheimer's Disease. Journal of Agricultural and Food Chemistry. 2019; 67: 10048–10058.

[15] He B, Chen P, Yang J, Yun Y, Zhang X, Yang R, *et al.* Neuroprotective effect of 20(*R*)-ginsenoside Rg(3) against transient focal cerebral ischemia in rats. Neuroscience Letters. 2012; 526: 106–111.

[16] He B, Chen P, Xie Y, Li S, Zhang X, Yang R, *et al.* 20(*R*)-Ginsenoside Rg3 protects SH-SY5Y cells against apoptosis induced by oxygen and glucose deprivation/reperfusion. Bioorganic & Medicinal Chemistry Letters. 2017; 27: 3867–3871.

[17] Bederson JB, Pitts LH, Tsuji M, Nishimura MC, Davis RL, Bartkowski H. Rat middle cerebral artery occlusion: evaluation of the model and development of a neurologic examination. Stroke. 1986; 17: 472–476.

[18] Zhang S, Qin C, Cao G, Xin W, Feng C, Zhang W. Systematic Analysis of Long Noncoding RNAs in the Senescence-accelerated Mouse Prone 8 Brain Using RNA Sequencing. Molecular Therapy - Nucleic Acids. 2016; 5: e343.

[19] Yemisci M, Eikermann-Haerter K. Aura and Stroke: relationship and what we have learnt from preclinical models. The Journal of Headache and Pain. 2019; 20: 63.

[20] Yang Q, Huang Q, Hu Z, Tang X. Potential Neuroprotective Treatment of Stroke: Targeting Excitotoxicity, Oxidative Stress, and Inflammation. Frontiers in Neuroscience. 2019; 13: 1036.

[21] Liu J, Zhang K, Hu B, Li S, Li Q, Luo Y, *et al.* Systematic Analysis of RNA Regulatory Network in Rat Brain after Ischemic Stroke. BioMed Research International. 2018; 2018: 8354350.

[22] Bao M, Szeto V, Yang BB, Zhu S, Sun H, Feng Z. Long non-coding RNAs in ischemic stroke. Cell Death & Disease. 2018; 9: 281.

[23] Zhang J, Yuan L, Zhang X, Hamblin MH, Zhu T, Meng F, *et al.* Altered long non-coding RNA transcriptomic profiles in brain microvascular endothelium after cerebral ischemia. Experimental Neurology. 2016; 277: 162–170.

[24] Sullenger BA, Nair S. From the RNA world to the clinic. Science. 2016; 352: 1417–1420.

[25] Deng Q, Li S, Wang H, Sun H, Zuo L, Gu Z, *et al.* Differential long noncoding RNA expressions in peripheral blood mononuclear cells for detection of acute ischemic stroke. Clinical Science. 2018; 132: 1597–1614.

[26] Rodrigo R, Fernández-Gajardo R, Gutiérrez R, Matamala JM, Carrasco R, Miranda-Merchak A, *et al.* Oxidative stress and pathophysiology of ischemic stroke: novel therapeutic opportunities. CNS & Neurological Disorders Drug Targets. 2013; 12: 698–714.

[27] Pisoschi AM, Pop A. The role of antioxidants in the chemistry of oxidative stress: a review. European Journal of Medicinal Chemistry. 2015; 97: 55–74.

[28] Verma N, Singh H, Khanna D, Rana PS, Bhadada SK. Classifica-

tion of drug molecules for oxidative stress signalling pathway. IET Systems Biology. 2019; 13: 243–250.
[29] Vallée A, Lecarpentier Y. Crosstalk between Peroxisome Proliferator-Activated Receptor Gamma and the Canonical WNT/$\beta$-Catenin Pathway in Chronic Inflammation and Oxidative Stress during Carcinogenesis. Frontiers in Immunology. 2018; 9: 745.
[30] Yao W, Huang J, He H. Over-expressed LOC101927196 suppressed oxidative stress levels and neuron cell proliferation in a rat model of autism through disrupting the Wnt signaling pathway by targeting FZD3. Cellular Signalling. 2019; 62: 109328.
[31] Kim J, Cho SY, Cho D, Kim SH, Seo DB, Shin SS. Oxidative Stress & FoxO Transcription Factors in Cardiovascular Aging. Current Medicinal Chemistry. 2017; 24: 943–949.
[32] Deng A, Ma L, Zhou X, Wang X, Wang S, Chen X. FoxO3 transcription factor promotes autophagy after oxidative stress injury in HT22 cells. Canadian Journal of Physiology and Pharmacology. 2021; 99: 627–634.
[33] Chen W, Zhang L, Zhou Z, Ren Y, Sun L, Man Y, *et al.* Effects of Long Non-Coding RNA LINC00963 on Renal Interstitial Fibrosis and Oxidative Stress of Rats with Chronic Renal Failure via the Foxo Signaling Pathway. Cellular Physiology and Biochemistry. 2018; 46: 815–828.
[34] Wu Y, Huang Y, Cai J, Zhang D, Liu S, Pang B. LncRNA SNHG12 Improves Cerebral Ischemic-reperfusion Injury by Activating SIRT1/FOXO3a Pathway through i nhibition of Autophagy and Oxidative Stress. Current Neurovascular Research. 2020; 17: 394–401.
[35] Anrather J, Iadecola C. Inflammation and Stroke: an Overview. Neurotherapeutics. 2016; 13: 661–670.
[36] Zhang F, Yan C, Wei C, Yao Y, Ma X, Gong Z, *et al.* Vinpocetine Inhibits NF-κB-Dependent Inflammation in Acute Ischemic Stroke Patients. Translational Stroke Research. 2018; 9: 174–184.
[37] Zhang Z, Li X, Chen F, Li Z, Wang D, Ren X, *et al.* Downregulation of LncRNA Gas5 inhibits apoptosis and inflammation after spinal cord ischemia-reperfusion in rats. Brain Research Bulletin. 2021; 168: 110–119.
[38] Zhao JH, Wang B, Wang XH, Wang JR, Xu CW. Influence of lncRNA ANRIL on neuronal apoptosis in rats with cerebral infarction by regulating the NF-κB signaling pathway. European Review for Medical and Pharmacological Sciences. 2019; 23: 10092–10100.
[39] Xu Q, Deng F, Xing Z, Wu Z, Cen B, Xu S, *et al.* Long non-coding RNA C2dat1 regulates CaMKIIδ expression to promote neuronal survival through the NF-κB signaling pathway following cerebral ischemia. Cell Death & Disease. 2016; 7: e2173.
[40] He W, Wei D, Cai D, Chen S, Li S, Chen W. Altered Long Non-Coding RNA Transcriptomic Profiles in Ischemic Stroke. Human Gene Therapy. 2018; 29: 719–732.
[41] Wu Z, Wu P, Zuo X, Yu N, Qin Y, Xu Q, *et al.* LncRNA-N1LR Enhances Neuroprotection against Ischemic Stroke Probably by Inhibiting p53 Phosphorylation. Molecular Neurobiology. 2017; 54: 7670–7685.
[42] Wen Y, Zhang Z, Li Z, Liu G, Tao G, Song X, *et al.* The PROK2/PROKR2 signaling pathway is required for the migration of most olfactory bulb interneurons. Journal of Comparative Neurology. 2019; 527: 2931–2947.
[43] Hexige S, Guo J, Ma L, Sun Y, Liu X, Ma L, *et al.* Expression pattern of growth/differentiation factor 3 in human and murine cerebral cortex, hippocampus as well as cerebellum. Neuroscience Letters. 2005; 389: 83–87.
[44] Li Q, Liu X, Wu Y, An J, Hexige S, Ling Y, *et al.* The conditioned medium from a stable human GDF3-expressing CHO cell line, induces the differentiation of PC12 cells. Molecular and Cellular Biochemistry. 2012; 359: 115–123.
[45] Liao L, Zhang M, Gu Y, Sun X. Targeting CCL20 inhibits subarachnoid hemorrhage-related neuroinflammation in mice. Aging. 2020; 12: 14849–14862.